JOURNAL OF THERMOPHYSICS AND HEAT TRANSFER
Vol. 6, No. 2, April–June 1992

Laminar Coupled Flow Downstream of an Asymmetric Sudden Expansion

George C. Vradis* and Lara VanNostrand†
Polytechnic University, Farmingdale, New York 11735

The effect of the expansion ratio and temperature varying viscosity on the hydrodynamic and heat transfer characteristics of the laminar flowfield over a backward facing step is studied numerically. Both walls are maintained at uniform but different temperatures, while the flow at the step is assumed to be hydrodynamically and thermally fully developed. Calculations are carried out for different Reynolds numbers in the laminar flow regime and for a Prandtl number of 5.3. It is shown that an increase in the expansion ratio results in the augmentation of the heat transfer coefficient along both walls, the augmentation becoming substantial at high expansion ratios. Empirical correlations are obtained for the average Stanton number in the recirculating zone as a function of the Reynolds number and the expansion ratio. The variation of viscosity with temperature is shown to have a substantial effect on both the reattachment length and the local Nusselt number distribution along both the step and flat walls, the effect becoming stronger as the Reynolds number increases.

Introduction

THE analysis of the convection heat transfer problem in separated-reattached flow fields is important in many practical applications, including heat exchangers, electronic boards, and combustors. It is well established that there is a large variation of the local heat transfer coefficient within separated flow regions and that substantial overall heat transfer augmentation may result in the region of reattachment. Improved understanding and numerical modeling of such flows can provide engineers with better prediction tools for solving design problems.

The simplest possible geometry involving a reattaching shear layer is the flow over a backward facing step. It offers an advantage in that the separation point is fixed by the geometry of the problem and independent of the flow characteristics while the resulting hydrodynamic and temperature fields remain as complex as in more involved geometries. The isothermal laminar flow problem has been extensively studied and documented, both experimentally (Armaly et al.[1]) and numerically (Armaly et al.,[1] Bentson and Vradis,[2] Kim and Moin,[3] and Thangam and Knight[4]). The isothermal turbulent flow problem has also been studied extensively (see Vogel and Eaton[5] for details).

The laminar forced convection heat transfer problem over a backward facing step has been studied experimentally by Aung[6] for uniform wall temperature and very small expansion ratios, corresponding practically to external flow conditions. The Nusselt number along the step wall attains a very low value at the separation point growing monotonically through the reattachment point. Downstream of reattachment the Nusselt number behaves as in a developing laminar boundary layer. No distinctive heat transfer property was associated with the reattachment point, but it was always located upstream of the point of maximum heat transfer coefficients. The average Stanton number in the recirculating zone increases with step height, the variation being very close to linear in the range of step heights studied. Oosthuisen and Paul[7] studied the problem numerically in the case of a fully or partially heated step wall.

The corresponding turbulent flow problem has been studied farily extensively for relatively small expansion ratios.[5,8] Vogel and Eaton[5] in their study for the turbulent flow case, concluded that different physical mechanisms determine the value of the heat transfer coefficient in different flow regions. Upstream of reattachment as the laminar-like boundary layer grows toward the center of the recirculation bubble the temperature gradient drops rapidly. The turbulence intensity in the reattachment region determines the value of the temperature gradients, whereas far downstream of reattachment the local skin friction coefficient determines the temperature gradients, in agreement with Reynolds analogy. Vogel and Eaton[5] also found the maximum Stanton number to vary as the -0.4 power of the Reynolds number.

In the case of substantially large expansion ratios, the nature of the problem changes from an external to an internal one. In the laminar flow regime the pressure gradient due to the flow expansion assumes an important role in the development of the hydrodynamic and thermal characteristics of the flowfield. For moderate to high Reynolds numbers it results in the appearance of a recirculating bubble along the flat wall. This bubble has a profound effect on the nature of the flowfield, changing it from two-dimensional to a three-dimensional one, even for very large aspect ratios.[1]

The assumption of constant fluid properties is acceptable in cases of small overall temperature differences, and for fluids with weak property dependence on temperature, as in the case with air. In most experimental studies, the working fluid has been air with small temperature differences in order to minimize free convection effects. Thus, these studies fall into the category of constant property flows.

The objective of this work is to study numerically the effect of expansion ratio in the constant property heat transfer problem as well as the effect of temperature varying viscosity on the flowfield and heat transfer rates over a two-dimensional, confined backward facing step. The incoming flow is assumed to be hydrodynamically and thermally fully developed. The step and flat walls are kept at different but uniform temperatures. The calculations are carried out for a Prandtl number equal to 5.3, that of water. In the case of constant properties, five different expansion ratios *ER* (defined as the ratio of the

Received Aug. 27, 1990; presented as Paper 91-0162 at the AIAA 29th Aerospace Sciences Meeting, Reno, NV, Jan. 7–10, 1991; revision received June 7, 1991; accepted for publication June 18, 1991.

*Assistant Professor of Mechanical Engineering. Member AIAA.
†Honors Student; currently Graduate Student, Department of Mechanical Engineering, California Institute of Technology, Pasadena, CA.

step height to the downstream channel height) of 0.25, 0.33, 0.5, 0.66, and 0.75 are studied. Of all the properties relevant to this problem, the dynamic viscosity is the water property with the strongest dependence upon temperature. (As an example, for a temperature range between 15°–60°C, while the specific heat, the density, and the thermal conductivity remain practically constant (they change less than 8%), the viscosity changes by more than 50%. It is, thus, obvious that the variation of the viscosity with temperature is the predominant variable property effect. The same is true for a large family of engine oils. Given that the viscous heating terms are negligible in this analysis, the maximum and minimum temperatures encountered in the field will be along the channel walls. The corresponding maximum and minimum values of the viscosity will be along the walls, also. Two cases of maximum to minimum viscosity ratio are studied; those of 2.34 and 3.86.

The study is based on the use of a fully second order accurate, strongly implicit, finite difference formulation of the governing elliptic equations, developed by Vradis,[9] which has already been shown[2] to be highly accurate and computationally efficient in the case of isothermal flows. The method is extended here to solve nonisothermal flows as well.

Governing Equations

The governing equations for the two dimensional, steady, laminar, incompressible flow of a Newtonian fluid in nondimensionalized form are

$$\frac{\partial u}{\partial x} + \frac{\partial v}{\partial y} = 0 \tag{1}$$

$$u\frac{\partial u}{\partial x} + v\frac{\partial u}{\partial y} = -\frac{\partial p}{\partial x} + \frac{1}{Re}\left\{\frac{\partial}{\partial x}\left[2\mu\frac{\partial u}{\partial x}\right] + \frac{\partial}{\partial y}\left[\mu\left(\frac{\partial u}{\partial y} + \frac{\partial v}{\partial x}\right)\right]\right\} \tag{2}$$

$$u\frac{\partial v}{\partial x} + v\frac{\partial v}{\partial y} = -\frac{\partial p}{\partial y} + \frac{1}{Re}\left\{\frac{\partial}{\partial y}\left[2\mu\frac{\partial v}{\partial y}\right] + \frac{\partial}{\partial x}\left[\mu\left(\frac{\partial u}{\partial y} + \frac{\partial v}{\partial x}\right)\right]\right\} \tag{3}$$

$$u\frac{\partial \theta}{\partial x} + v\frac{\partial \theta}{\partial y} = \frac{1}{Pe}\left[\frac{\partial^2\theta}{\partial x^2} + \frac{\partial^2\theta}{\partial y^2}\right] \tag{4}$$

where x, y are the nondimensional, with respect to the upstream channel height a, streamwise and transverse coordinates, $u = U/U_0$, $v = V/U_0$, $p = P/(\rho U_0^2)$ are the nondimensionalized velocities and pressure respectively, $\theta = (T - T_{wc})/(T_{wh} - T_{wc})$ is the nondimensionalized temperature (T_{wh} is the temperature of the hot wall while T_{wc} is the temperature of the cold wall) and $\mu = \bar{\mu}/\mu_0$ is the nondimensionalized viscosity with respect to the viscosity corresponding to the minimum temperature in the field. The Reynolds number $Re = 2\,a\,\rho\,U_0/\mu_0$ is based on the average velocity U_0 of the incoming flow at the step, twice the height a of the upstream channel, which is equal to the hydraulic diameter of the channel, and the viscosity μ_0 of the fluid for the minimum temperature encountered in the field and the Peclet number is $Pe = RePr$ (where Pr is the Prandtl number), which is constant in all cases because it is independent of the viscosity.

Solution Technique

A set of finite difference equations is used to approximate the system of partial differential Eqs. (1–4) in the present work. The well-known staggered grid proposed by Welch et al.[10] for the Marker and Cell (MAC) method is employed (see Fig. 1). The formulation is fully second-order accurate. Second-order accurate upwind differencing is used to descretize the convective derivatives in the main flow direction (x direction) to warranty stability. Second-order accurate centered differences are used for all other terms. The resulting system of algebraic equations is as follows:

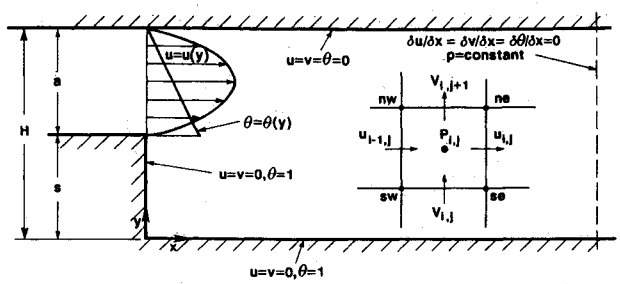

Fig. 1 Backward facing step: geometry and boundary conditions.

$$\frac{u_{i,j} - u_{i-1,j}}{\Delta x} + \frac{v_{i,j+1} - v_{i,j}}{\Delta y} = 0 \tag{5}$$

$$\hat{u}_{i,j}\frac{3u_{i,j} - 4u_{i-1,j} + u_{i-2,j}}{2\Delta x} + v_{av}\frac{u_{i,j+1} - u_{i,j-1}}{2\Delta y} = -\frac{\hat{p}_{i+1,j} - p_{i,j}}{\Delta x} + \frac{1}{Re}\frac{1}{\Delta x}\left[2\,\mu_{i+1,j}\frac{u_{i+1,j} - u_{i,j}}{\Delta x} - 2\,\mu_{i,j}\frac{u_{i,j} - u_{i-1,j}}{\Delta x}\right] + \frac{1}{Re}\frac{1}{\Delta y}\left[\mu_{ne}\frac{u_{i,j+1} - u_{i,j}}{\Delta y} - \mu_{se}\frac{u_{i,j} - u_{i,j-1}}{\Delta y} + \mu_{ne}\frac{\hat{v}_{i+1,j+1} - v_{i,j+1}}{\Delta x} - \mu_{se}\frac{\hat{v}_{i+1,j} - v_{i,j}}{\Delta x}\right] \tag{6}$$

$$u_{av}\frac{3v_{i,j} - 4v_{i-1,j} + v_{i-2,j}}{2\Delta x} + \hat{v}_{i,j}\frac{v_{i,j+1} - v_{i,j-1}}{2\Delta y} = -\frac{p_{i,j} - p_{i,j-1}}{\Delta y} + \frac{1}{Re}\frac{1}{\Delta y}\left[2\,\mu_{i,j}\frac{v_{i,j+1} - v_{i,j}}{\Delta y} - 2\,\mu_{i,j-1}\frac{v_{i,j} - v_{i,j-1}}{\Delta y}\right] + \frac{1}{Re}\frac{1}{\Delta x}\left[\mu_{se}\frac{v_{i+1,j} - v_{i,j}}{\Delta x} - \mu_{sw}\frac{v_{i,j} - v_{i-1,j}}{\Delta x} + \mu_{se}\frac{u_{i,j} - u_{i,j-1}}{\Delta y} - \mu_{sw}\frac{u_{i-1,j} - v_{i-1,j-1}}{\Delta y}\right] \tag{7}$$

$$u_{av}\frac{3\theta_{i,j} - 4\theta_{i-1,j} + \theta_{i-2,j}}{2\Delta x} + \hat{v}_{i,j}\frac{\theta_{i,j+1} - \theta_{i,j-1}}{2\Delta y} = \frac{1}{Pe}\frac{\theta_{i,j+1} - 2\theta_{i,j} + \theta_{i,j-1}}{\Delta y^2} + \frac{1}{Pe}\frac{\hat{\theta}_{i+1,j} - 2\theta_{i,j} + \theta_{i-1,j}}{\Delta x^2} \tag{8}$$

where

$$v_{av} = \frac{\hat{v}_{i+1,j} + \hat{v}_{i,j} + \hat{v}_{i+1,j+1} + \hat{v}_{i,j+1}}{4}$$

$$u_{av} = \frac{\hat{u}_{i,j} + \hat{u}_{i,j-1} + u_{i-1,j-1} + u_{i-1,j}}{4}$$

and the viscosity $\mu_{i,j}$ is defined at the same point with the pressure.

The above set of equations is written for constant x and y grids, but it can easily be rewritten for variable grids. In the "up-winded" terms the differencing is done based on the sign of the corresponding velocity that multiplies the term. A positive velocity results in backward differencing (as shown in Eqs. (5–8)), whereas a negative velocity results in "forward" differencing. The viscosity μ is defined at the same point with the pressure. The indices *ne*, *nw*, *se*, and *sw* indicate the four corners of the grid element.

The resulting system of algebraic equations is a nonlinear one. It is linearized by adopting an iterative solution technique (described by Vradis[11]) and evaluating the coefficients of the convective derivatives at the previous iteration level (indicated by a circumflex above the variables).

As is obvious from the governing equations, the only possible coupling of the momentum equations with the energy equation is through the viscosity. In the case where the viscosity is constant, the hydrodynamic problem is completely independent of the thermal problem. As a result, the continuity and momentum equations are solved first, simultaneously. Once the velocity field has been obtained to the desired level of accuracy, the energy equation, which is linear, is solved for the temperature distribution. Only a small number of iterations is usually required for the converged solution to be obtained.

In the case of temperature varying viscosity, however, the momentum and energy equations are coupled. Therefore, all four equations are solved simultaneously. The values of the viscosity are updated at the end of each iteration, based on the newly obtained temperature distribution. This results in an increase in both the required computational time and in the required number of iterations. For both cases, however, the solution technique results in a very robust, efficient, and strongly implicit alogrithm. The results presented here were obtained using a 60 × 48 grid, which was nonuniform in both directions. In Case II (see next section) and for the higher Reynolds numbers, a 70 × 48 grid was used in order to accommodate for the increase in the length of the developing flow region. Grids of these sizes were required in order to obtain grid-independent solutions to engineering accuracy.

Problem

The geometry and the boundary conditions of the problem are shown in Fig. 1. In the case of the constant property flow, five different expansion ratios s/H have been chosen; 0.25, 0.33, 0.5, 0.66, and 0.75. The flow at the step is assumed to be fully developed, both hydrodynamically and thermally. Thus, the velocity profile is parabolic,[12] whereas the temperature profile is linear because viscous dissipation effects are neglected. At the exit, which is always located far downstream so that the flow there is fully developed, the streamwise derivatives of the velocity components and the temperature are set to zero, while the pressure remains uniform. The required location of the downstream boundary for the results to be independent of its position is not known a-priori. It depends both on the expansion ratio and the Reynolds number. Numerical experimentation was required to determine the appropriate size of the computational domain. The position of this boundary depends heavily on the Reynolds and Peclet numbers. As both numbers increase, the size of the computational domain required for the exit boundary condition to be accurate, increases. As an example, for $Re = 50$ the exit is located at 42 step heights away, for $Re = 400$ at 170 step heights away, and for $Re = 800$ at 275 step heights away. Along the solid walls the velocities are zero, while the nondimensional temperature is zero along the flat wall, and one along the step wall. In the numerical implementation of the boundary conditions while the transverse component of the velocity and the temperature are located on the physical boundary, the streamwise component is not. A parabolic distribution of this component of the velocity is assumed next to the wall, which results in an exact representation of the velocity profile in the fully developed flow region and a second order accurate one in the rest of the field.

The temperature varying viscosity problem is solved for an expansion ratio of 0.5. The flow at the step is again assumed to be fully developed, both hydrodynamically and thermally. Therefore, the temperature profile is again linear because viscous heating effects are neglected in the present analysis. The fully developed velocity profile at the step is not parabolic any more and is obtained numerically by solving the hydrodynamic entrance flow problem between two parallel plates, using the same code. At the exit, the flow is assumed fully developed, allowing the streamwise derivatives of the velocities and the temperature to be set to zero, while the pressure remains uniform. As mentioned above in the constant property case, it was always verified after every run that the downstream boundary was located far enough from the step so that the flow there was completely fully developed. Along the solid walls the velocities are zero, while the nondimensional temperature is either zero or one, depending upon the case. There are two thermal boundary conditions that have been employed in the course of this work. The first one, referred to as Case I hereafter, involves a lower viscosity for the step wall, i.e. $\theta = 1$ for the step wall and $\theta = 0$ for the flat wall. The second one, referred to as Case II hereafter, involves a lower viscosity for the flat wall, i.e. $\theta = 0$ for the step wall and $\theta = 1$ for the flat wall.

The viscosity of the fluid, which is assumed to be water, is calculated at different temperatures by the following formula:

$$\ell n\left(\frac{\bar{\mu}}{\mu_0}\right) = a_1 + a_2\frac{T_0}{T} + a_3\frac{T_0^2}{T^2} \tag{9}$$

where $a_1 = -1.94$, $a_2 = -4.8$, and $a_3 = 6.74$ as given by White[13] (T in Kelvin and μ in kg/(m·s)).

A particular difficulty in obtaining generalized solutions to this problem is that although a large number of fluids behave according to Eq. (9), a different set of constants has to be used for each one of them. Further study is needed to predict the behavior of other fluids in order to generalize such results.

Results

Constant Viscosity

Results are given for Reynolds numbers in the range of 50 to 800. The code has been validated by comparing the hydrodynamic solution to existing experimental and numerical calculations. Figure 2 shows the predicted reattachment length as a function of the Reynolds number as compared to the experimental and numerical results of Armaly et al.[1] and the

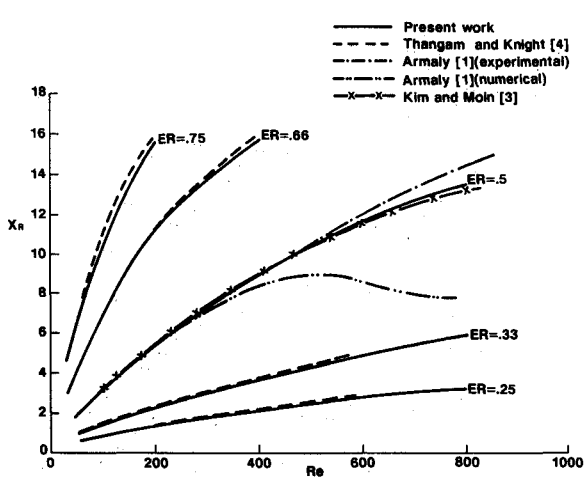

Fig. 2 Reattachment length vs Reynolds number for constant viscosity case.

numerical solutions of Kim and Moin[3] and Thangam and Knight.[4] For $ER = 0.5$ the agreement with the experimental data is excellent up to $Re = 500$. For higher Reynolds numbers the numerical results, although they still predict the general trends, deviate from the experimental values, a fact attributed to the apparent three dimensionality of the flowfield in this Reynolds number range, as demonstrated in the experiments performed by Armaly et al.[1] For the other expansion ratios, the agreement with the numerical results of Thangam and Knight[4] is very good, although there is a definite trend for their predictions to be consistently slightly higher than those of the present work.

As seen in Fig. 2, the calculation for expansion ratios 0.66 and 0.75 was terminated at Reynolds numbers 400 and 200, respectively. The reason for this is that the flow goes into transition at these Reynolds numbers, as indicated by the lack of convergence to a solution for Reynolds numbers higher than these (It is a well-established fact that steady-state numerical codes fail to converge when the flow goes into transition). For $ER = 0.5$ the experimental results of Armaly et al.[1] indicate that transition occurs at $Re = 1200$, whereas the code fails to converge at $Re > 1150$. For the smaller expansion ratios transition occurs at higher Reynolds numbers.

Another interesting aspect of this flow configuration is the appearance of a separation region along the flat wall in a certain range of Reynolds numbers. The experimental results available for $ER = 0.5$ show the appearance of this region at $Re = 450$, accompanied by three-dimensional effects that become stronger as the Reynolds number increases. The discrepancy of the numerical results for the reattachment length from the experimental values for $Re > 500$ is generally attributed to these three-dimensional effects. The Reynolds number at which separation along the flat wall appears decreases as the expansion ratio increases. This is expected given that the adverse pressure gradient generated by the expansion increases as the expansion ratio increases.

Figures 3 through 7 show the predicted Nusselt number distributions along the step and flat walls for the five different expansion ratios respectively, for Reynolds numbers of 50, 200, and 400 for $ER = 0.25$, 0.33, and 0.5 and of 50, 133, and 200 for $ER = 0.66$ and 0.75 (all Nusselt numbers are based on the upstream channel height). Here x is the axial distance measured from the step. In all cases, the Nusselt number along the step wall is very small at the separation point and it grows as the reattachment point is approached. As seen, however, there is a substantial qualitative difference in the Nusselt number distribution between the two smaller

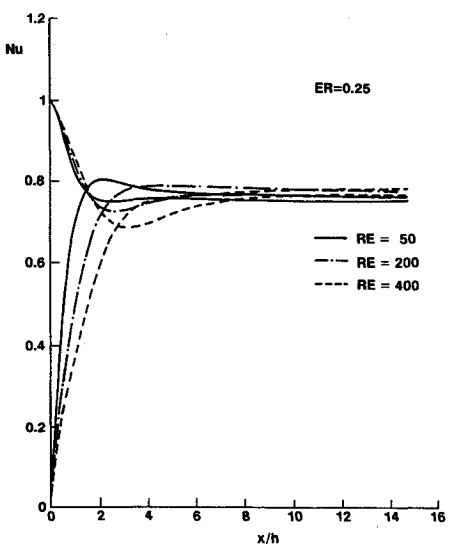

Fig. 3 Nusselt number distribution along step and flat walls for constant viscosity and $ER = 0.25$.

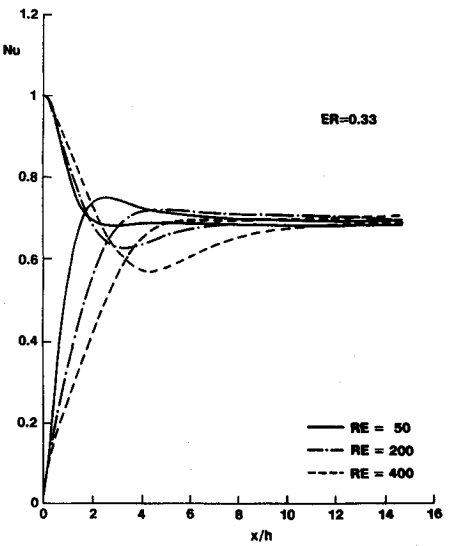

Fig. 4 Nusselt number distribution along step and flat walls for constant viscosity and $ER = 0.33$.

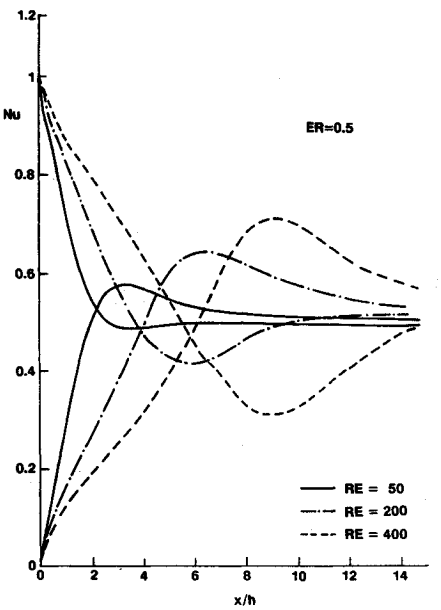

Fig. 5 Nusselt number distribution along step and flat walls for constant viscosity and $ER = 0.5$.

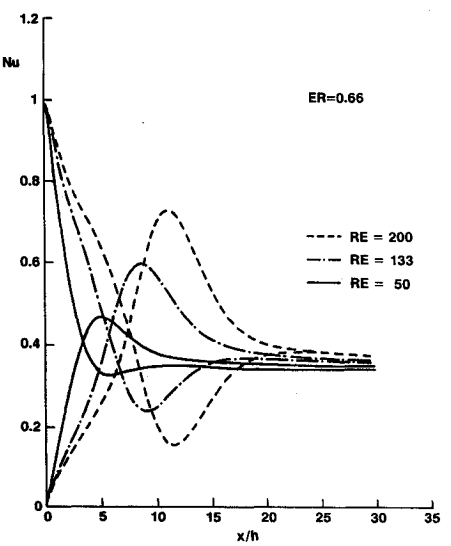

Fig. 6 Nusselt number distribution along step and flat walls for constant viscosity and $ER = 0.66$.

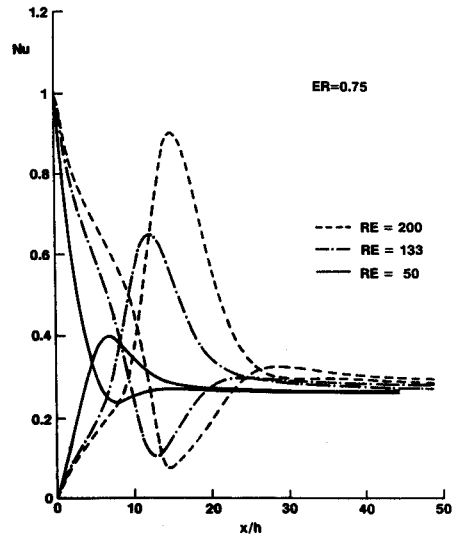

Fig. 7 Nusselt number distribution along step and flat walls for constant viscosity and $ER = 0.75$.

expansion ratios and the three higher ones. In the case of the two smaller expansion ratios, the reattachment point is not related to any distinctive heat transfer characteristics, as has been also verified by Aung.[6] In the case of the three higher expansion ratios the reattachment point is the point of a local maximum for the heat transfer coefficient, the maximum value increasing with an increase in the Reynolds number. Downstream of the reattachment point the Nusselt number drops gradually to the constant value corresponding to the fully developed flow regime. It is obvious that the Reynolds analogy fails completely in this case because the Stanton number reaches a maximum at the point of zero skin friction (reattachment point).

Along the flat wall the flow develops as a laminar boundary layer, its thickness depending upon the Reynolds number and the pressure gradient. As is well established,[12] laminar boundary layers are extremely sensitive to adverse pressure gradients. The adverse pressure gradient in the separation region increases both with the Reynolds number and the expansion ratio. As a result the thickness of the boundary layer along the flat wall in that region grows and, consequently, the heat transfer coefficient drops. Downstream of reattachment the pressure gradient becomes negative, the boundary layer becomes thinner, and the Nusselt number increases gradually to its fully developed flow value. Along the flat wall the Reynolds analogy is shown here to be valid provided, of course, that the flow does not separate. The Nusselt number drops fairly rapidly reaching a minimum close to the reattachment point and then gradually increases to the fully developed flow value.

Figures 8 and 9 show the predicted Nusselt number distribution along the step and flat walls for Reynolds number 100 and for the five expansion ratios studied. Along the step wall there is a decrease both in the maximum Nusselt number and in the Nusselt number in the fully developed region of the flowfield as the expansion ratio increases. As a result, high expansion ratios are associated with decreased levels of heat transfer coefficients and increased augmentation. As seen, however, at very high expansion ratios the augmentation is so severe that the maximum Nusselt numbers in the cases of $ER = 0.66$ and 0.75 are practically equal. Correspondingly, along the flat wall the minimum Nusselt number decreases with increasing expansion ratio, resulting in the decreased heat transfer rates associated with the higher expansion ratios.

For external flows over cavities, Chapman[14] indicates that the average Stanton number in a cavity varies with the inverse of the square root of the Reynolds number. For the unconfined backward-facing step problem, despite its differences

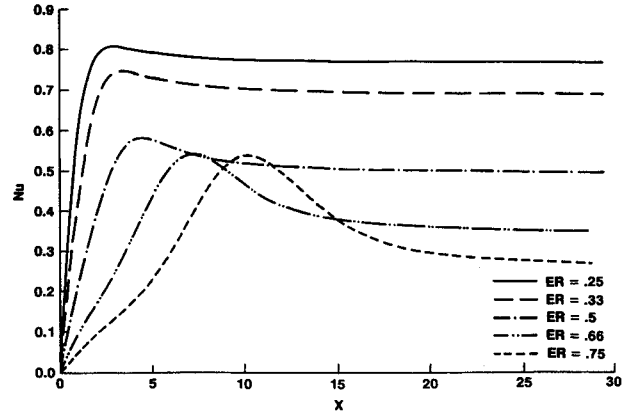

Fig. 8 Nusselt number distribution along step wall for $Re = 100$, constant viscosity, and different expansion ratios.

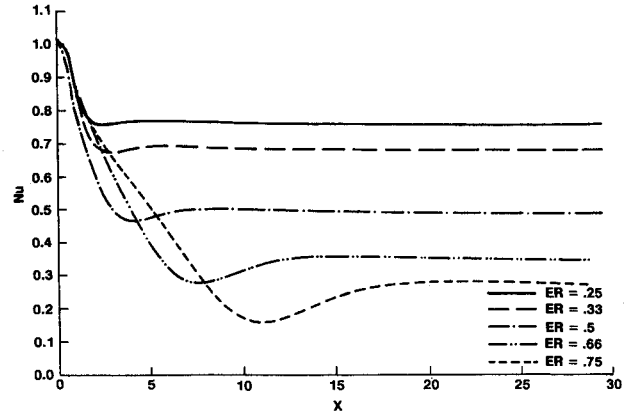

Fig. 9 Nusselt number distribution along flat wall for $Re = 100$, constant viscosity, and different expansion ratios.

from Chapman's analysis, the similarities provided the rational for a comparison, as worked out by Aung.[6] Aung's experimental results indicate that in his case, the average Stanton number varies with the Reynolds number according to the following equation:

$$\overline{St}_s = c_1 Re^{-.55} \tag{10}$$

where c_1 depends upon the step height. In the case of the confined step studied here, the following correlation is obtained for the average Stanton number in the recirculating flow region:

$$\overline{St}_s = c_1 Re^{-c_2} \tag{11}$$

where c_1 and c_2 are functions of the expansion ratio as given in Table 1. Equation (11), with the values given in Table 1, predicts the numerical data within 6%. These results indicate that although the functional dependence of the average Stanton number on the Reynolds number is similar for the cases of the unconfined and the confined backward-facing steps, the actual constants are very different.

Variable Viscosity, Case I

In Case I the viscosity along the step wall is smaller than the viscosity along the flat wall. Figure 10 shows the predicted reattachment length as a function of the Reynolds number for two cases of temperature varying viscosity ($\mu_{max}/\mu_{min} = 2.34$ and 3.86) as compared to the constant viscosity case. There is a substantial change in the reattachment length as compared to the constant viscosity case. The higher the maximum to minimum viscosity ratio, the higher the reattachment length for the same Reynolds number.

Table 1 Constants for Eq. (11)

Expansion ratio	c_1	c_2
0.25	0.022	0.881
0.33	0.031	0.865
0.5	0.052	0.838
0.66	0.063	0.727
0.75	0.041	0.559

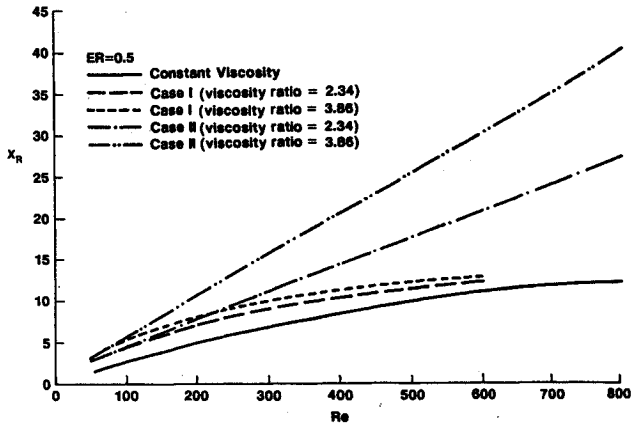

Fig. 10 Reattachment length vs Reynolds number for variable viscosity cases.

The Nusselt number distributions along the step and flat walls are shown in Figs. 11 and 12, respectively, and for the two maximum to minimum viscosity ratios. The points of maximum and minimum Nusselt number have been shifted downstream so that they appear in the immediate vicinity of the reattachment point again. At the same time, an increase in the maximum Nusselt number along the step wall is evident, accompanied by a decrease in the minimum Nusselt number along the flat wall. At low Reynolds numbers these changes are not significant but as the Reynolds number increases they become quite substantial. The larger the maximum to minimum viscosity ratio, the larger the increase (decrease) of the maximum (minimum) Nusselt number. As an example, for $Re = 200$ and $\mu_{max}/\mu_{min} = 3.86$, the changes in the maximum Nusselt number along the step wall and the minimum Nusselt number along the flat wall as compared to the constant viscosity case are 28% and 48%, respectively.

Because in this case the viscosity along the step wall is smaller than that along the flat wall, the local "effective" Reynolds number (defined using the local value of the viscosity coefficient) along the edge of the recirculation zone and the redeveloping boundary layer is actually higher than the prescribed one (which is based on the highest value of the viscosity in the field). As a result the reattachment length and the local Nusselt numbers are higher than in the constant viscosity case. On the other hand, along the flat wall the boundary layer experiences not only an adverse pressure gradient as in the constant viscosity flow, but in addition a negative viscosity gradient in the transverse direction. As is well established (Schlichting[12]), such a gradient results in a rapid growth in the boundary-layer thickness and the development of a point of inflection in the streamwise velocity profile. This results in the further decrease in the minimum Nusselt number in the vicinity of the reattachment point. The corresponding average Stanton and Nusselt numbers within the recirculating zone along the step wall have increased, as compared to the constant viscosity case. This is also attributed to the increase of the local "effective" Reynolds number.

Another aspect of the flow, also of great interest, is the appearance of a separation bubble along the flat wall. As mentioned earlier, in the case of the constant property flow, a recirculation bubble appears along the flat wall for Reynolds

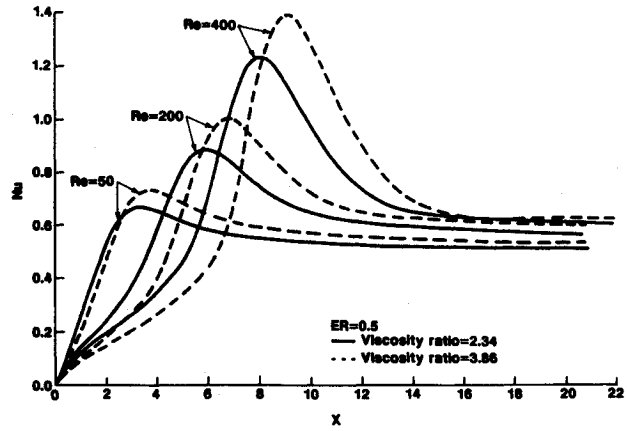

Fig. 11 Nusselt number distribution along step wall for case I.

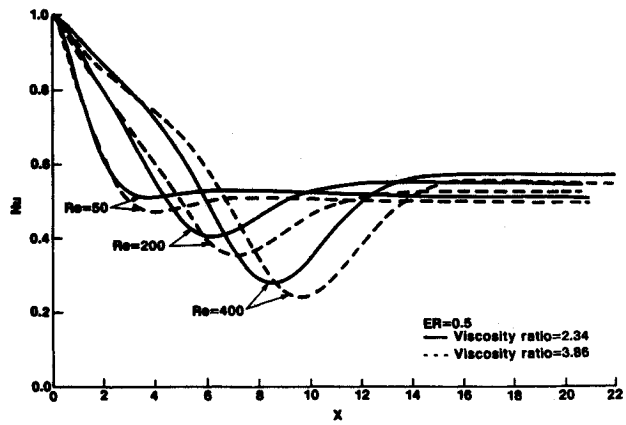

Fig. 12 Nusselt number distribution along flat wall for case I.

numbers greater than 450. The appearance of this separated flow region has a significant effect on the nature of the flow, changing it from a two-dimensional to a three-dimensional one (Armaly et al.[1]). As a result, the solutions obtained by two-dimensional codes deviate from experimental results, the discrepancy being larger with increasing Reynolds numbers. Two-dimensional codes predict the appearance of this separated flow region but fail to predict its location with accuracy. The heating of the step wall results in a negative viscosity gradient within the flat wall boundary layer. As mentioned earlier, a negative viscosity gradient within a boundary layer introduces an inflection point in the streamwise velocity profile and makes it unstable, the flow eventually separating much earlier than in the constant viscosity case. Thus, the bubble appears at a Reynolds number of about 250 for $\mu_{max}/\mu_{min} = 2.34$ and 150 for $\mu_{max}/\mu_{min} = 3.86$, which is substantially lower than in the constant property flow case ($Re = 450$).

Variable Viscosity, Case II

In Case II the viscosity along the step wall is higher than the viscosity along the flat wall. Figure 10 shows the predicted reattachment length as a function of the Reynolds number for the two viscosity ratios employed in this analysis and compares them to the constant viscosity case. The reattachment lengths for Case II are much larger than those for both the constant viscosity case and Case I. As in Case I, the higher the maximum to minimum viscosity ratio, the higher the reattachment length for the same Reynolds number. The decrease of the skin friction along the flat wall due to the decrease in viscosity, and the corresponding displacement of the streamlines closer to that wall, allows for the growth of the recirculating bubble along the step wall and the increase in the reattachment length.

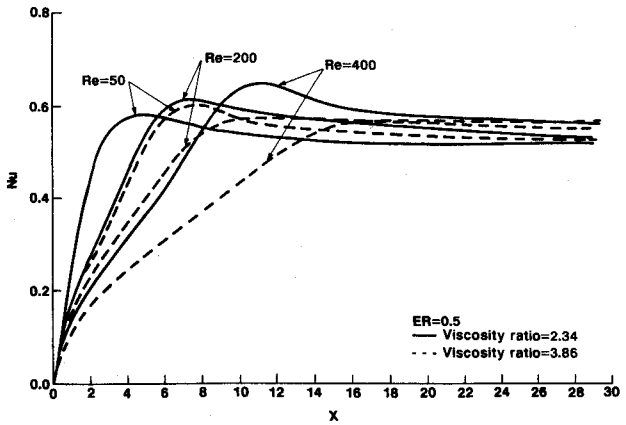

Fig. 13 Nusselt number distribution along step wall for case II.

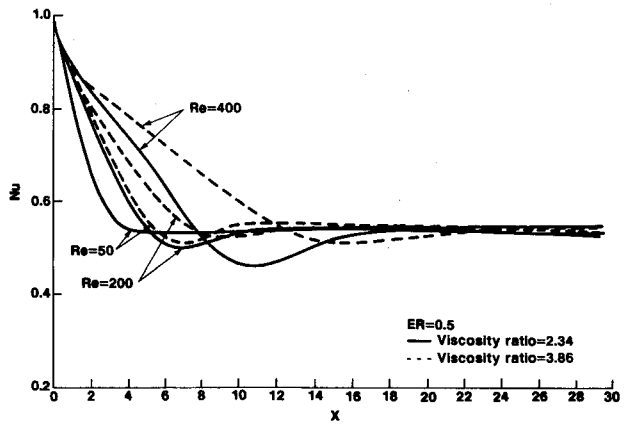

Fig. 14 Nusselt number distribution along flat wall for case II.

The Nusselt number distributions along the step and flat wall are shown in Figs. 13 and 14, respectively. As seen, the Nusselt number along both the step and the flat walls still exhibits local maximum and minimum values correspondingly, but the augmentation is much weaker than that in the constant viscosity case and in Case I. Along the flat wall, given the decrease in the viscosity of the fluid and the positive viscosity gradient, the boundary layer becomes thinner and as a result the minimum Nusselt number increases as compared to the constant viscosity case and Case I. Because the viscosity of the fluid away from the step wall is substantially smaller than that close to the wall, the Nusselt number distribution along the step wall exhibits the behavior encountered in the unconfined step flow where there is not any distinctive heat transfer property associated with the reattachment point (see Aung[6]) and the Nusselt number varies monotonically from very small values at the step to the fully developed flow value.

Therefore, the decrease of the viscosity along the flat wall has a profound effect on the thermal aspect of the flow. It results in an augmentation of the local heat transfer coefficient much less substantial than that present in the other two cases studied. Because of the decrease of the local maximum in the Nusselt number along the step wall, the average Stanton number in the recirculating zone is lower than in the other cases studied.

Another interesting result of the heating of the flat wall, is the disappearance of the separation bubble along that wall for the entire range of Reynolds numbers studied up to transition. In this case, as indicated earlier, because the viscosity gradient within the flat wall boundary layer is positive, a more stable boundary layer is obtained and separation is avoided completely.

Conclusions

The basic aspects of the heat transfer problem in the case of laminar flow over a backward-facing step have been studied using a second-order accurate, strongly implicit, finite difference algorithm. Both walls of the channel are kept at uniform but different temperatures. In the case of the constant property flow, at low expansion ratios the Nusselt number along the step wall varies practically monotonically from very small values at the step to the corresponding fully developed Nusselt number downstream, in agreement to the experimental results obtained by Aung for very small expansion ratios. As the expansion ratio increases the Nusselt number distribution along the step wall exhibits a local maximum at the immediate vicinity of the reattachment point. This maximum value decreases rapidly with increasing expansion ratio. Along the flat wall the same distribution always exhibits a local minimum in the immediate vicinity of the reattachment point and varies overall in good agreement with the Reynolds analogy. The average Stanton number in the recirculation zone varies with the Reynolds number following the general law of open cavities, with the actual constants in the equation depending upon the expansion ratio. In the case of variable viscosity, the reattachment length increases compared to the constant viscosity case. The increase is larger in the case where the viscosity along the flat wall is smaller than that along the step wall. For both thermal boundary conditions, the increase in the reattachment length is larger as the maximum to minimum viscosity ratio increases. Lower viscosity along the step wall results in the appearance of the recirculation bubble along the flat wall at Reynolds numbers smaller than in the constant property flow. In the case of lower viscosity along the flat wall, a profound change in the hydrodynamic and thermal structure of the flow takes place. The flow along the flat wall does not separate at all and the Nusselt number drops gradually from its value at the step to that corresponding to the thermally fully developed flow. As a result the heat transfer coefficient augmentation is most important in Case I, whereas it is minimal in Case II.

Acknowledgment

This research work was partially supported by the Pittsburgh Supercomputing Center through Grant MSM890007P, which provided the necessary computing resources. Its support is hereby greatly acknowledged.

References

[1]Armaly, B. F., Durst, F., Pereira, J. C. F., and Schonung, B., "Experimental and Theoretical Investigation of Backward Facing Step Flow," *Journal of Fluid Mechanics*, Vol. 127, 1983, pp. 473–496.

[2]Bentson, J., and Vradis, G., "A Two-Stage Pressure Correction Technique for the Incompressible Navier-Stokes Equations," *AIAA Journal*, Vol. 28, No. 7, 1991, pp. 1155–1156. Also published as AIAA Paper 87-0545.

[3]Kim, J., and Moin, P., "Application of a Fractional Step Method to Incompressible Navier-Stokes Equations," *Journal of Computational Physics*, Vol. 59, No. 2, 1985, pp. 308–323.

[4]Thangam, S., and Knight, D., "Effect of Step Height on the Separated Flow Past a Backward Facing Step," *Physics of Fluids A: Fluid Dynamics*, Vol. 1. No. 3, 1989, pp. 701–707.

[5]Vogel, J. C., and Eaton, J. K., "Combined Heat Transfer and Fluid Dynamic Measurements Downstream of a Backward Facing Step," *Journal of Heat Transfer*, Vol. 107, Nov. 1985, pp. 922–929.

[6]Aung, W., "An Experimental Study of Laminar Heat Transfer Downstream of Backsteps," *Journal of Heat Transfer*, Vol. 105, Nov. 1983, pp. 823–829.

[7]Oosthuizen, P. H., and Paul, J. T., "Laminar Forced Convective Heat Transfer from a Heated Wall Section Downstream of a Rearward Facing Step," *Collected Papers in Heat Transfer*, HTD-Vol. 123, American Society of Mechanical Engineers, 1989.

[8]Shishov, E. V., Roganov, P. S., Grabarnik, S. I., and Zabolotsky, V. P., "Heat Transfer in the Recirculating Region Formed by a Backward Facing Step," *International Journal of Heat and Mass Transfer*, Vol. 31, No. 8, 1988, pp. 1557–1562.

[9]Vradis, G., "Acceleration Techniques for the Solution of the Incompressible Navier-Stokes Equations," Ph.D Dissertation, Polytechnic University, Farmingdale, NY, 1987.

[10]Welch, J. E., Harlow, F. H., Shannon, J. P., and Daly, B. J., "The MAC Method," Los Alamos Scientific Lab, Rept. LA-3425, 1966.

[11]Vradis, G., "The Effect of Expansion Ratio on the Heat Transfer in Laminar Flow Downstream of a Backward Facing Step," AIAA Paper 91-0162, AIAA 29th Aerospace Sciences Meeting, Reno, NV, Jan. 7–10, 1991.

[12]Schlichting, H., *Boundary—Layer Theory*, 7th ed., McGraw-Hill, New York, 1979.

[13]White, F. M., *Fluid Mechanics*, 2nd ed., McGraw Hill, New York, 1986, p. 28.

[14]Chapman, D. R., "A Theoretical Analysis of Heat Transfer in Regions of Separated Flow," NACA TN 3792, 1956.